Influence of Mixing Cycle on the Degree of Mixing of Calcite-Filled Polyethylene Upon Stretching

Kwang-Jea Kim,[1,*] Sangmin Kwon,[1] Hyun Kim,[1] Patit P. Kundu,[1] Yong-Wook Kim,[2,*] Yong-Keun Lee,[2,*] Kyu Jong Lee,[2,*] Byung H. Lee,[2] Soonja Choe[1]

[1]*Department of Chemical Engineering, Inha University, Inchon 402-751, South Korea*
[2]*Taedok Institute of Technology, SK Corporation, Taejon 305-370, South Korea*

Received 27 July 2001; accepted 29 April 2002

ABSTRACT: The mixing cycle-dependent degree of dispersion and degree of mixing of a calcite (calcium carbonate) agglomerate in high-density polyethylene (HDPE), low-density polyethylene (LDPE), and linear low-density polyethylene (LLDPE) matrices upon stretching was investigated using three different techniques: mechanical property, morphological behavior, and image analyzer analyses. The mechanical properties analyzed in terms of the tensile strength and maximum elongation resulted in that the second mixing was the best for giving a better property for all systems except the LDPE system, which exhibited no significant difference between the second and third mixings. The morphological behavior of the three compounds were different, but no distinctive difference was observed to differentiate the degree of mixing from system to system. The number-, weight-, and $z + 1$-average diameters of the air hole and the aspect ratio upon the stretching and mixing cycle were calculated to analyze the degree of mixing of the calcite-filled composites. As a consequence, no difference in the average diameter of the air hole was obtained among the three systems, but the aspect ratios of the air hole varied significantly. Thus, the degree of dispersion and the degree of mixing may be influenced by the average calcite agglomerate size, the average diameter of the air hole, and the aspect ratio upon stretching and mixing cycles. Those factors would be formed by the difference in chemical characteristics upon various microstructures of polyethylene and its molecular weight and molecular weight distribution. © 2003 Wiley Periodicals, Inc. J Appl Polym Sci 87: 311–321, 2003

Key words: polyethylene (PE); composites; zeolite dispersions; microstructure

INTRODUCTION

Mineral particles treated with interfacial agents such as stearic acids or silane tend to wet or lubricate particle surfaces, followed by yielding a lower viscosity than that of untreated particles since the treated ones more easily slide past each other than do the untreated ones, resulting in reduced interparticle forces, reduced viscosity, and less agglomeration.[1] Anisotropic particles such as fibers and flakes are easily oriented to the flowing direction, yielding reduced particle–particle interactions at high shear.[2] Some additives such as sulfur-added silane coupling agents[3] and acrylamide[4] bond the particles and the polymer, strongly yielding an increase in viscosity.

The addition of mineral particles causes a significant increase in the viscosity of a compound. Among them, calcite is the most abundant mineral as a reinforcing particle in the thermoplastic industry. Compounding calcite into the thermoplastic matrix was studied by various researchers.[4–12] A few studies were employed on the stretching flow of these compounds[2,5,7] using minerals such as carbon black, calcium carbonate, and titanium dioxide and it was reported that similar behavior occurred at low strain rates.

Wetting between polymers was studied in terms of the factors such as contact angle, surface tension, interfacial tension, and polarity.[13,14] When the contact angle becomes zero or less than zero, it indicates wetting of the particles, which is often expressed as the critical surface tension. On the other hand, dewetting occurs when the surface of a particle is covered with a low surface tension material such as impurities or adsorbed water layers.[15] Since most engineering thermoplastics have a higher surface tension, their use in combination with materials having a low surface tension may result in dewetting or crack formation.

Coating calcite with chemicals was studied by various researchers.[2,5,7,8] Stearic acid has been known to improve the processability in calcite-filled thermoplastics[2,5,8]; however, the disadvantage of using this is the moisture absorption of calcite.[2,9] A calcite surface grafted by acrylamide was reported to improve the mechanical property of the high density polyethylene (HDPE) composite.[2] All those works were focused on improving the processing property. The particle size

Correspondence to: S. Choe (sjchoe@inha.ac.kr).
**Present address:* Struktol Company of America, Stow, OH
Contract grant sponsor: SK Corp.
Contract grant sponsor: Inha University; contract grant number: KRF-99-E013.

TABLE I
PEs Used in This Study

Olefin (grade name)	Density (g/cm^3)	MI (g/10 min)	HDT (°C)	Tensile strength (kg/cm^2)	Code
High-density polyethylene (3300)	0.954	0.8	123	350	HDPE
Low-density polyethylene (FB300)	0.919	3.0	90	120	LDPE
Linear low-density polyethylene (FT810)	0.918	2.1	98	350	LLDPE

MI, melt index; HDT, heat-distortion temperature.

of the filler after mixing depends mainly on the processing conditions. There were experimental studies of fiber breakage and its relationship upon processing conditions.[6–20] Shon and White compared the particle-size reduction in various types of a continuous mixer.[20]

In the previous report,[21] we first investigated the tensile and rheological properties using HDPE/$CaCO_3$, *low-density polyethylene* (LDPE)/$CaCO_3$, and *linear low-density polyethylene* (LLDPE)/$CaCO_3$ composites and found that each system exhibited a reinforcing effect due to the incorporation of calcite into pure polyethylene (PE). The composite systems exhibited dewetting and a formation of an air hole as well as factors controlling the air-hole size and shape. We also studied the morphology through SEM to investigate air-hole formation and its mechanism using stretched film specimens.

In the present article, the objective was to investigate the degree of dispersion and the degree of mixing of calcite particles in various PE systems using HDPE/$CaCO_3$, LDPE/$CaCO_3$, and LLDPE/$CaCO_3$ upon the mixing cycles. The analysis used three different techniques: mechanical tests, morphological observation, and image-analyzer analysis using scanning electron microscopy (SEM) photographs. In particular, the degree of mixing is quantitatively rationalized by comparing the experimental results and the theoretical equations.

EXPERIMENTAL

Materials

Three different olefins and a calcite were used. The olefins used in this study were HDPE, LDPE, and LLDPE supplied by the SK Corp. (Ulsan, South Korea). The calcite used in this study was stearic acid-coated SST-40 supplied by the DOWA Corp. (Tokyo, Japan) and its average particle size and BET surface area were 1.1 μm and 4.8 m^2/g. The PE composite with calcite had a 50:50 wt % ratio. Information of the materials used in this study is listed in Tables I and II.

Mixing

A Brabender PL 2000 twin-screw extruder (TSE) was used for compounding the calcite particles and HDPE, LDPE, and LLDPE with a 50:50 wt % ratio. Premixed calcite and polyolefins were fed into the extruder hopper and the compounded samples extruded through extruder die were pelletized (first mix); they were remixed in the same TSE (second mix), and the remixed pellets were again processed using the same TSE (third mix). A temperature gradient was maintained in the barrel of the extruder: 190°C at the feeding zone, 210°C at the compression zone, 220°C at the metering zone, and 230°C at die end for the HDPE system. The extruded materials were pelletized after passing through a water bath at 25°C. The operation temperature of the extruder was ambient from sample to sample (HDPE at 230°C, LDPE at 210°C, and LLDPE at 220°C) at 70 rpm.

Dumbbell bar and film preparation

The specimens with a dumbbell bar shape were prepared using a Carver laboratory hot press at 2×10^4 Pa and 200°C. Film specimens were also prepared using sheet extrusion at 200°C installed with a slit die (100×0.5 mm), which was attached at the end of the extruder. An extruded sheet was pulled out using a take-up device and the film thickness was maintained at 0.4 mm. The film specimen was prepared following ASTM D882-97, which had a dimension of 15×0.4 mm. The dimension of the dumbbell bar specimen was $13 \times 3 \times 165$ mm following ASTM D638, which had a dimension of 13×3 mm.

Characterization

Tensile test at constant strain rate

The stress–strain experiments using the dumbbell bar and film specimen were performed using an Instron 4301 at 20°C and 30% humidity. Both ends of the specimen were firmly tightened by an upper and a lower grip. The initial gap separation was 10 mm and the rate of elongation (the strain rate) was fixed at 5 mm/min for both the dumbbell bar and the film spec-

TABLE II
Calcite Used in This Study

Calcite (grade name)	Density (g/cm^3)	Particle size (μm)	BET area calculated (m^2/g)	Code (comment)
SST-40	2.9	1.1	4.8	Treated calcite

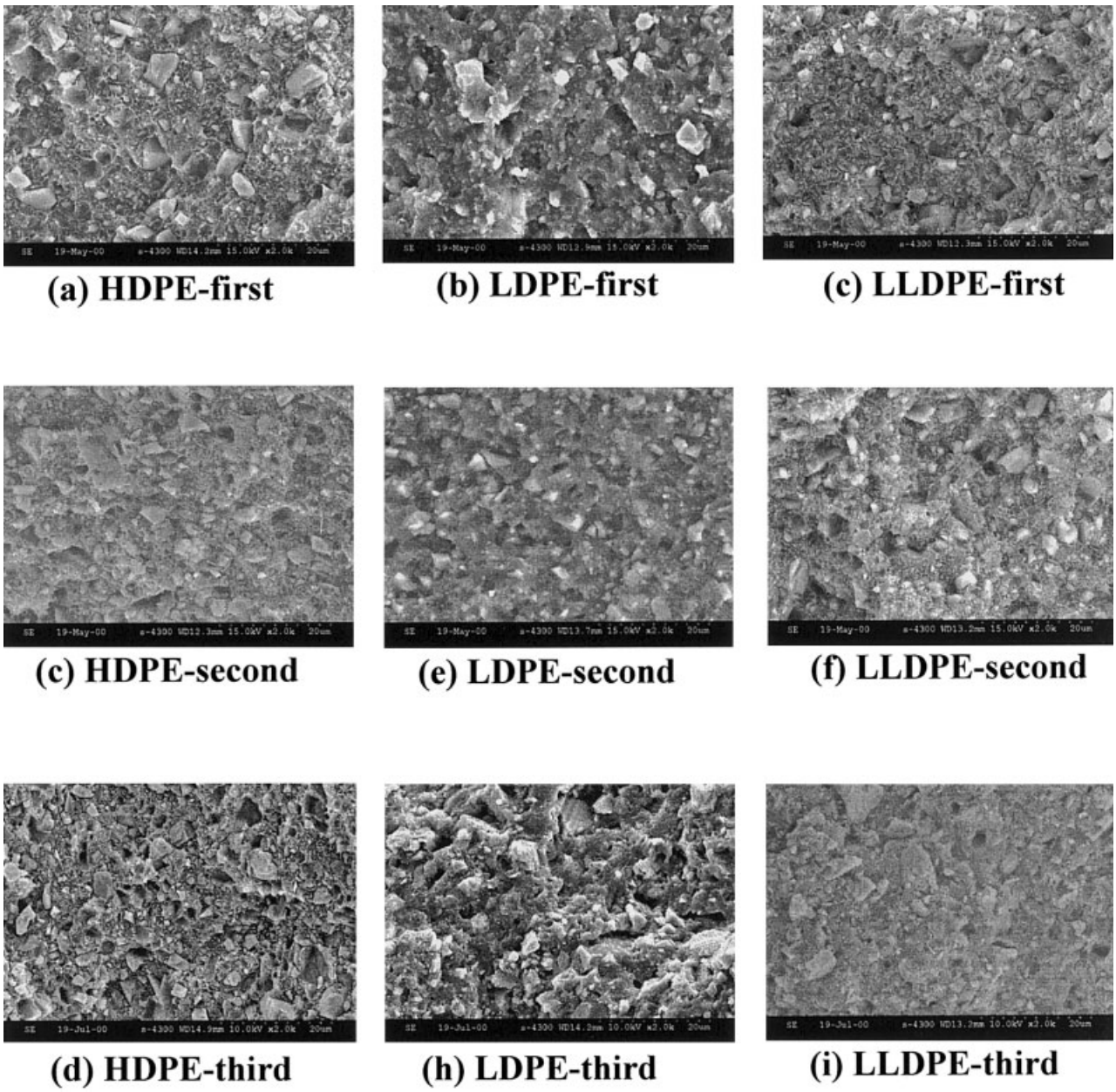

Figure 1 SEM photograph of the calcite-filled HDPE, LDPE, and LLDPE composites upon mixing cycles.

imens. The dumbbell specimen was slowly stretched from 25 to 50%, then from 50 to 100, 150, 200, 300, and 400% from sample to sample to study the morphological differences at various strain ratios. Thus, each stretched specimen was used for SEM observation and for further analysis of the image analyzer (IA).

Morphology and analysis using an IA

The prepared specimen was fractured in liquid nitrogen and coated with silver using a sputter coater. The morphology of the side surface of film and dumbbell bar was also studied after stretching the specimen at ambient strain ratios and the SEM photographs of each image were taken at 2000 magnification. A Hitachi S-4300 SEM was used to obtain the image of the fractured surface, the stretched specimen surface, and the particle agglomerate.

The dispersion of the calcite particle after stretching the specimens was investigated using a Hitachi S-4300 SEM photograph, and the size and the number of air holes were analyzed using an IA system, Leica LQ500MC. The air-hole diameter was calculated in terms of the number average (d_n), weight average (d_w), and z + 1 average (d_{z+1}) using to the following equations[22]:

$$d_n = \frac{\sum N_i d_i^1}{\sum N_i} \quad (1a)$$

$$d_w = \frac{\sum N_i d_i^3}{\sum N_i d_i^2} \quad (1b)$$

$$d_{z+1} = \frac{\sum N_i d_i^4}{\sum N_i d_i^3} \quad (1c)$$

where N_i is the number of air holes of the air-hole diameter and d_i, the diameter of the i-th particle.

RESULTS AND DISCUSSION

Figure 1 presents SEM photographs of the fractured parts of the calcite-filled HDPE, LDPE, and LLDPE composites upon mixing cycles from the first to third mixing. Although the SEM photograph is not clear, calcite seems to be wetted more in the PE matrix in the second and third mixings regardless of the systems. For the three systems, the face morphology of the HDPE, LDPE, and LLDPE systems showed a network-type matrix.

Figure 2 exhibits the analyzed number- and weight-average calcite diameter in the fractured dumbbell bar of the HDPE, LDPE, and LLDPE matrix as a function of the mixing cycles without stretching. Figure 2(a) exhibits that the number-average calcite diameter dramatically decreases with the mixing cycles in HDPE, but no significant difference between the first and the third mixings was observed in the LDPE and LLDPE systems. For the HDPE system, the number-average diameter of the calcite agglomerate disintegrates from 1.2 to 0.9 μm for the first to the third mixing; on the other hand, for the LDPE and LLDPE systems, it is 0.45–0.5 μm regardless of mixing cycle. In Figure 2(b), the weight-average calcite diameter decreases abruptly from 5 to 2 μm with the mixing cycles in HDPE, but that for the LDPE and LLDPE systems varied in a different way: The weight-average calcite agglomerate disintegrated from 1.2 to 0.9 μm and from 1.4 to 1.0 μm between the first and third mixing of LDPE and LLDPE, respectively. This may be due to the further breakup of calcite agglomerates in the TSE at high shear stress upon mixing. The breakdown of the calcite agglomerate was significant in HDPE compounds and the overall average calcite particle size in the HDPE system is two to three times larger than that of LLDPE and LDPE. In addition, in Figure 2(a), the number average of LDPE is slightly larger than that of LLDPE, but in Figure 2(b), the trend is reversed due to the presence of big particles in the LLDPE system. This sort of reversion is often observed when the particle-size distribution is wide; in particular, big particles affect the $z + 1$-average diameter.

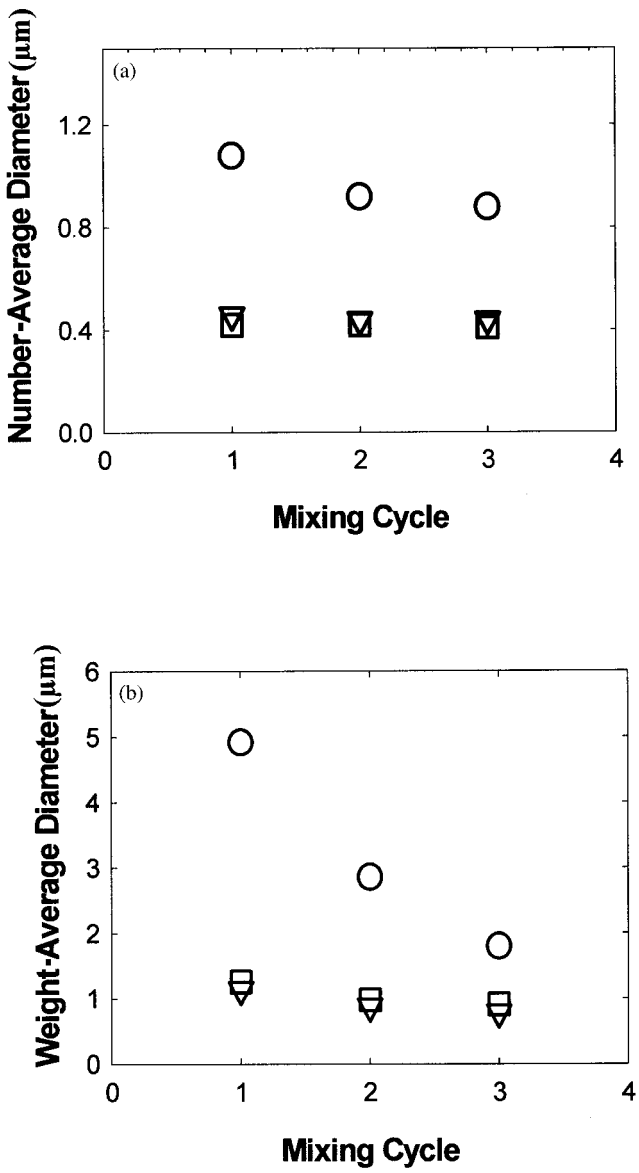

Figure 2 Number- and weight-average calcite diameter (μm) in the (○) HDPE, (▽) LDPE, and (□) LLDPE matrices as a function of mixing numbers without stretching.

Figure 3 represents the stress–strain curves of the calcite-filled HDPE dumbbell bar upon mixing cycle (the bar indicates the experimental error range). The maximum elongation at break for the first, second, and third mixing is 34, 60, and 37%, respectively. In addition, the average yield stress is 13.5, 14.5, and 14 MPa, respectively. In this figure, we used the maximum elongation rather than the tensile stress as the preference for the degree of dispersion and the degree of mixing of the calcite particles because we believe that the higher the elongation the better is the mixing between the filler and the matrix. Another factor counted for affecting the degree of mixing is the experimental error range. Thus, twice mixing of the HDPE/calcite composite was chosen to exhibit better

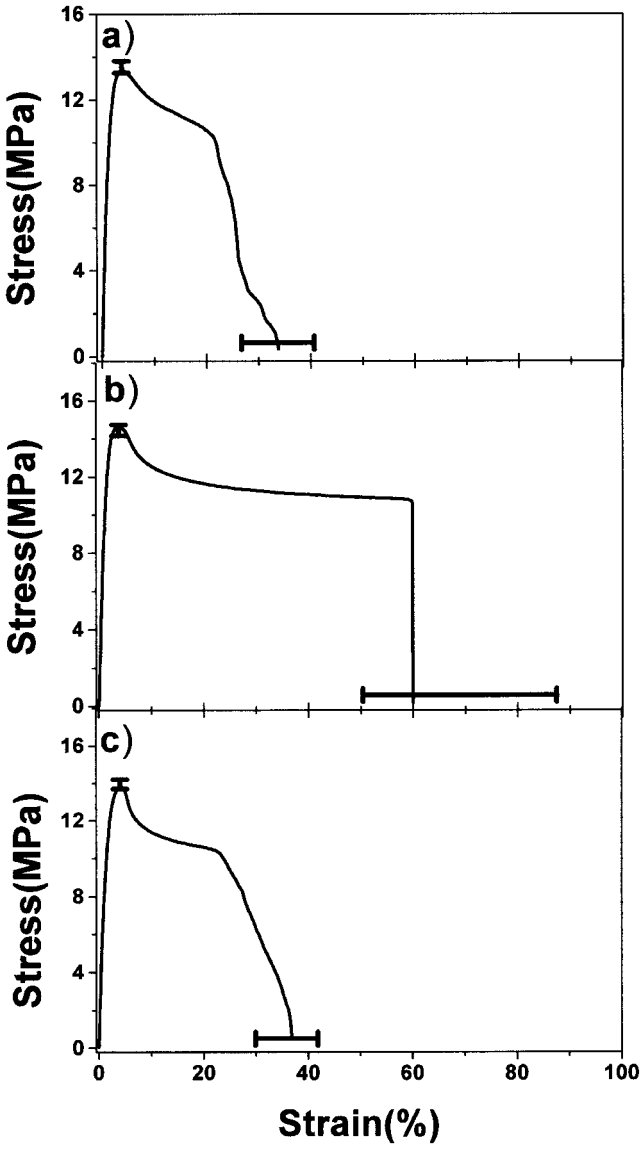

Figure 3 Stress–strain curve of calcite-filled HDPE dumbbell bar upon mixing (the bar indicates the experimental error range): (a) first mixing; (b) second mixing; (c) third mixing.

dispersion of the calcite in the HDPE matrix due to higher elongation among the three systems. This phenomenon may be related to the suitable calcite agglomerate size and its distribution in the matrix.

Figure 4 represents stress–strain curves of the calcite-filled LDPE dumbbell bar upon the mixing cycle. The maximum elongation at break upon the first, second, and third mixing cycles is 12.5, 18.2, and 18.2% and the yield stress is 8, 8.5, and 8.5 MPa, respectively. Thus, the second and the third mixing cycles exhibited the best tensile property. Concerning the experimental error bar, no difference between the second and third mixing gave a similar degree of mixing due to an uncountable error margin.

Stress–strain curves of the calcite-filled LLDPE dumbbell bar upon the mixing cycle are presented in Figure 5. Compared with the HDPE and LDPE systems, the LLDPE system seems to be strong in tearing strength. The maximum elongation at break for the first, second, and third mixing was 15, 55, and 40%, respectively, and the yield stress was 9–10 MPa regardless of the mixing cycle. Thus, the second mixing exhibited better tensile properties in the LLDPE system. From Figures 3–5, the second mixing seems to give a better degree of mixing and degree of dispersion of the calcite in the HDPE, LDPE, and LLDPE matrices.

The average diameter of the air hole was measured by converting the diameter of the elliptical air hole to the corresponding sphere as a function of the strain

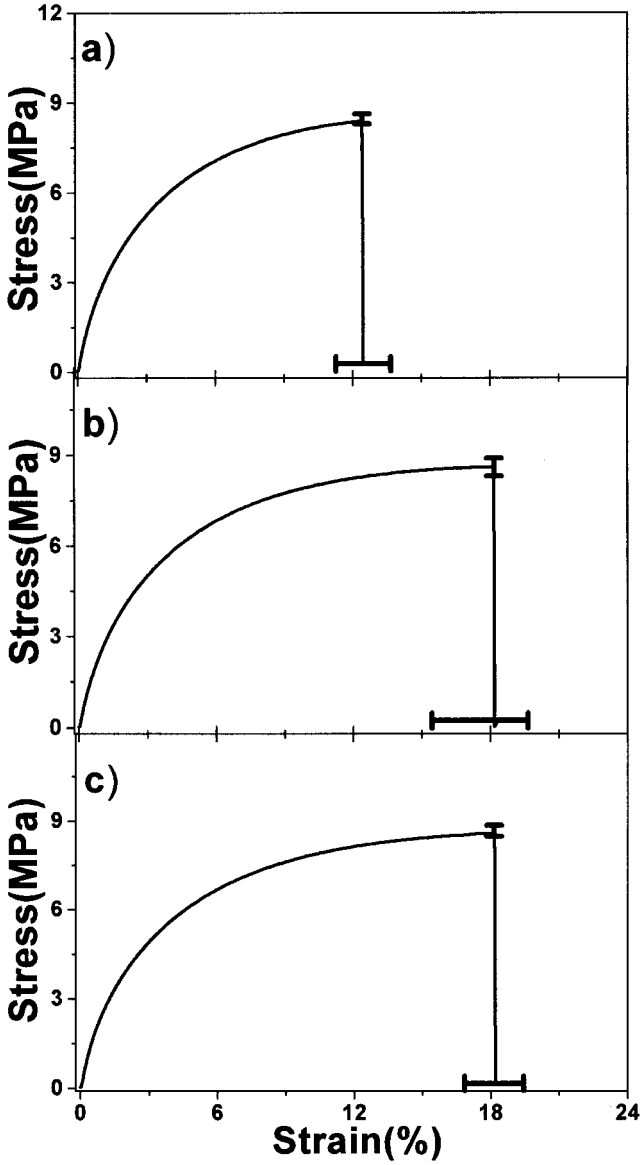

Figure 4 Stress–strain curve of calcite-filled LDPE dumbbell bar upon mixing (the bar indicates the experimental error range): (a) first mixing; (b) second mixing; (c) third mixing.

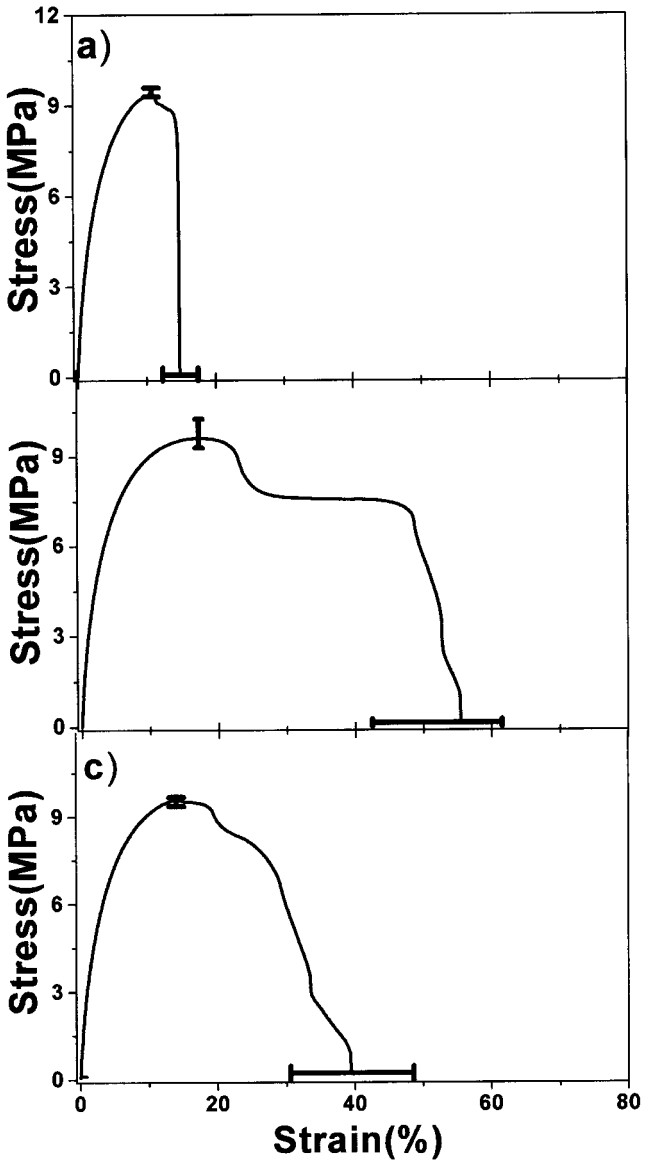

Figure 5 Stress–strain curve of calcite-filled LLDPE dumbbell bar upon mixing (the bar indicates the experimental error range): (a) first mixing; (b) second mixing; (c) third mixing.

ratio. According to eq. (1), the air-hole diameter was calculated in terms of the number-average, weight-average, and $z + 1$-average diameter. In Figure 6(a), we observed that the number average of the air-hole diameter increased from 0.5 to 1.2 μm with the strain ratio for HDPE, from 0.4 to 1.0 μm for LDPE, and from 0.4 to 1.3 μm for LLDPE upon stretching. On the other hand, the weight-average of the air-hole diameter in Figure 6(b) was from 0.6 to 1.5 μm for HDPE, from 0.7 to 1.3 μm for LDPE, and from 0.5 to 1.5 μm for LLDPE, which means that the weight average of the air-hole diameter gradually increased with the strain ratio. For the $z + 1$-average diameter, the air-hole sizes increased from 1.0 to 2.3 μm upon stretching for all three systems. From 0 to 50% of strain, the air hole was formed due to dewetting or slippage between the calcite and the PE matrix, but, thereafter, the air hole was enlarged due to breakage of the fibril structure of the matrix upon further stretching. The breakup of the calcite particles or agglomerates would be one of the factors forming enlarged air holes and dispersion of the calcite particles.

Figure 7 represents the stretched surface of the calcite-filled HDPE, LDPE, and LLDPE composites. Al-

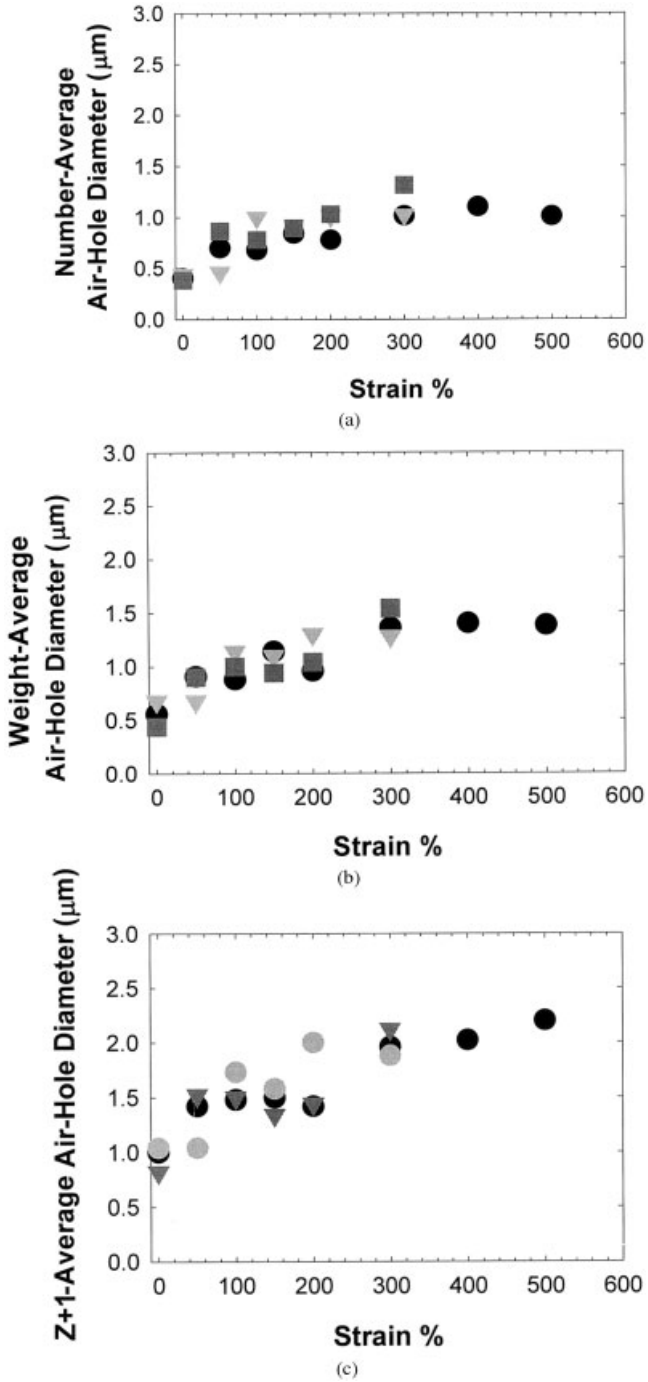

Figure 6 Air-hole diameter (μm) of calcite-filled (○) HDPE, (▽) LDPE, and (□) LLDPE composites due to strain: (a) number-average, (b) weight-average; (c) $z + 1$ average.

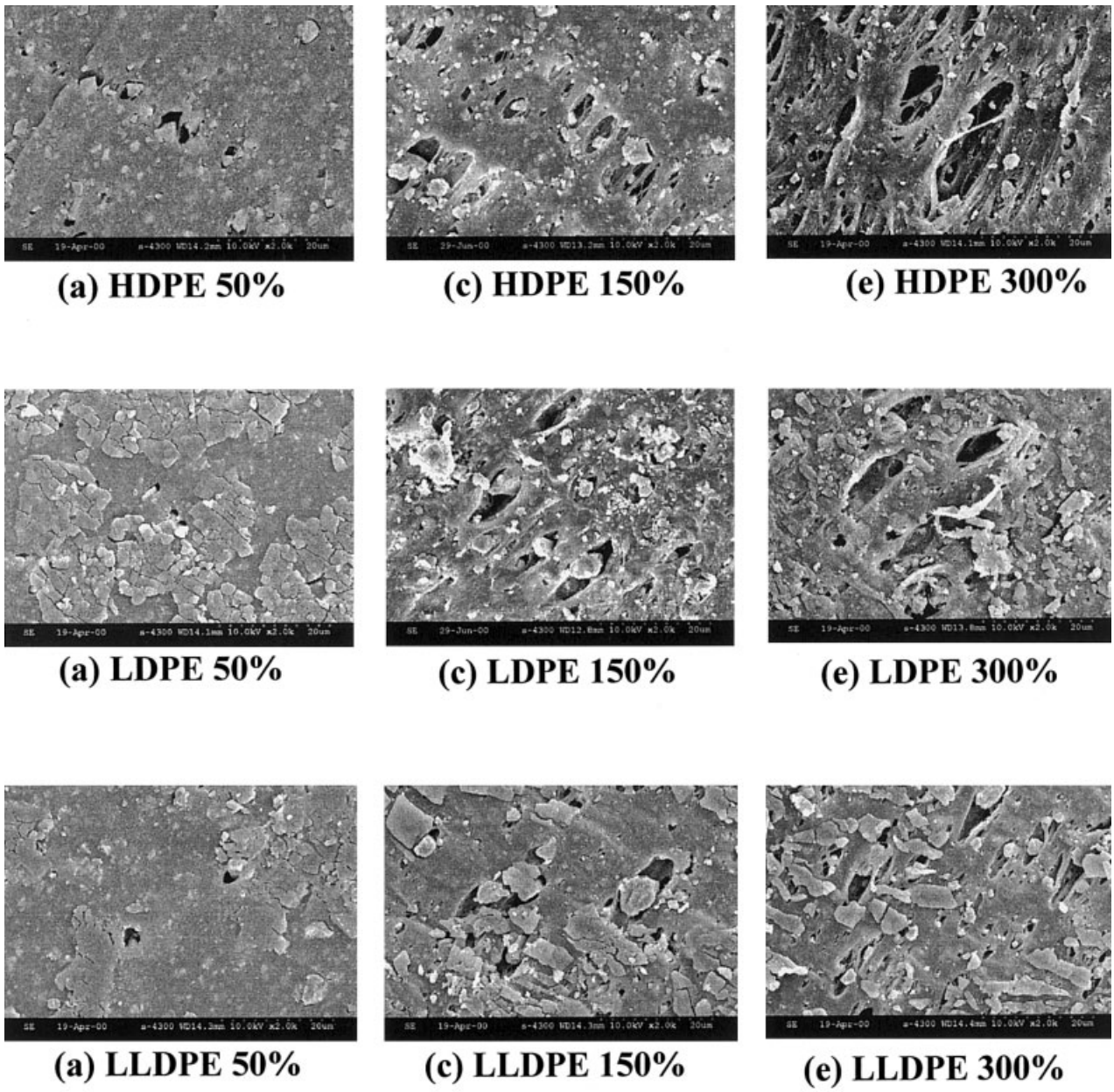

Figure 7 Stretched surfaces of the calcite-filled HDPE, LDPE, and LLDPE composites.

though it seems to show much larger air-hole sizes upon further stretching as seen in Figure 7, the average size of the air hole is more or less the same as seen in Figure 6; this may have arisen from the formation of a small air hole upon further stretching. The HDPE compound exhibited a further increase of the average air hole up to 400% of strain, then decreased at 500%. At 500% strain, many small air holes were formed between the HDPE fibrils. This may come from a combination of low molecular weight characteristics (short chain) of HDPE with a mid molecular weight distribution (MWD) or with a narrow MWD. A similar trend of small air-hole formation was observed for the LDPE and LLDPE systems. For the LDPE and LLDPE systems, the elongation was not enough compared to that of the HDPE system.

The air hole was quantitatively analyzed by the aspect ratio. Figure 8 represents the aspect ratio (the ratio of the longest length to the shortest length of the air hole) as a function of the strain ratio. Two different phenomena were obtained: The first was that the aspect ratio of the HDPE, LDPE, and LLDPE systems varied from 1.3 to 2.0, which is more or less the same up to 150% stretching. Then, that of the HDPE composite was abruptly increased from 2.5 to 7.5 upon straining from 200 to 400%. But as the strain ratio increased further to 500%, the aspect ratio decreased, presumably due to merging of the air hole. The aspect

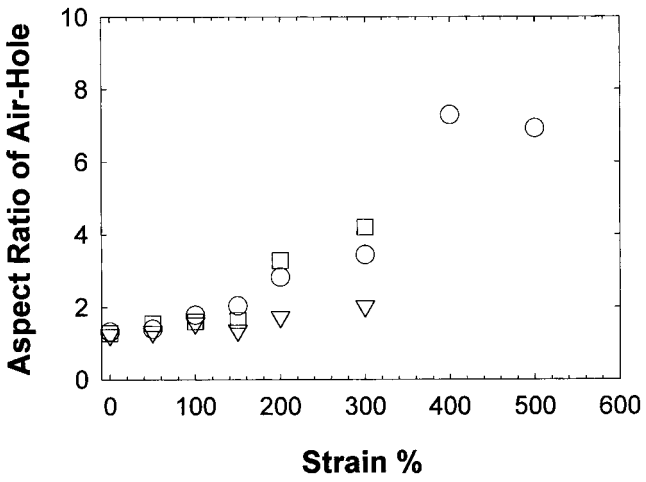

Figure 8 Aspect ratio of calcite-filled (○) HDPE, (▽) LDPE, and (□) LLDPE composites due to strain.

ratio of the LDPE and LLDPE systems was increased from 1.8 to 3 and from 3 to 6.1, respectively, which means that the air hole on further stretching was enlarged not only due to the breaking of the air hole, but also to the formation of the fibril structure of the HDPE matrix. In the previous report,[21] we suggested that the air-hole formation arose from the dewetting between the calcite particles and the matrix in the initial stretching (100–150% strain). However, in the later stage of stretching, the breaking fibril structure and the emerging effect influenced the formation of air holes. Thus, our present result agrees well with the previous report, because, in the beginning of the stretching up to 150%, there was no significant difference in the aspect ratio regardless the systems. Thus, various aspect ratios depending on the system would be affected by various factors such as the polymer characteristics, polymer chain orientation upon elon-

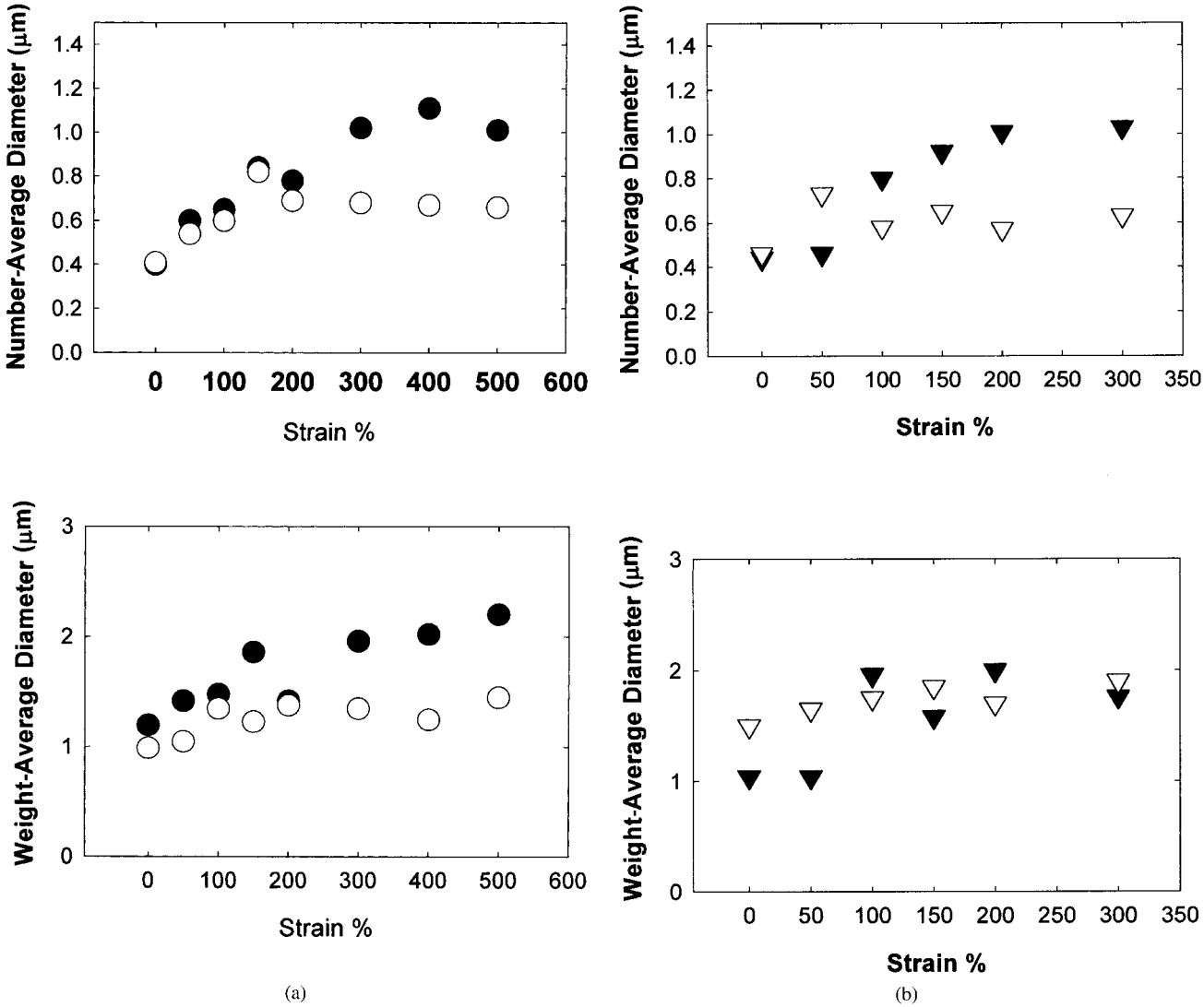

Figure 9 Number- and weight-average of air-hole diameter (μm) of calcite-filled compounds after (solid) second and (open) third mixings as a function of strain: (a) HDPE system; (b) LDPE system; (c) LLDPE system.

gation, or different molecular weight and MWD of each constituent.

The number- and weight-average of the air-hole diameter upon second and third mixing cycles is drawn in Figure 9(a) as a function of strain ratio of HDPE. The same number- and weight-average diameter of the LDPE and LLDPE composites are also drawn in Figure 9(b,c), respectively. This may relate to the calcite size reduction (narrow distribution) between the first and the third mixing cycle as seen in Figure 2. As the mixing cycle increases, the average calcite size decreases (especially between the first and second mixing) due to high mechanical shear stress in the TSE. The appearance of a small air hole without the presence of the air-hole initiator (calcite) lowered the average air hole size at the third mixing. This may due to the mechanical degradation of PE in the TSE as shown by the tensile curves shown in Figures 3 and 5. Overall, the second mixing of the three PE systems

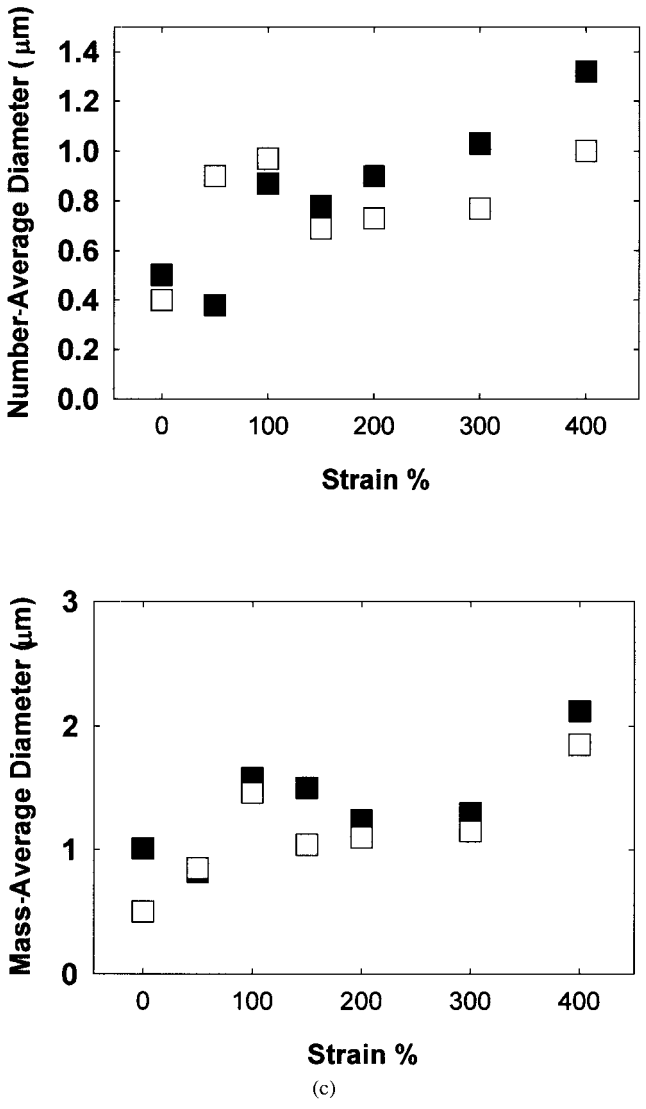

Figure 9 (*Continued from the previous page*)

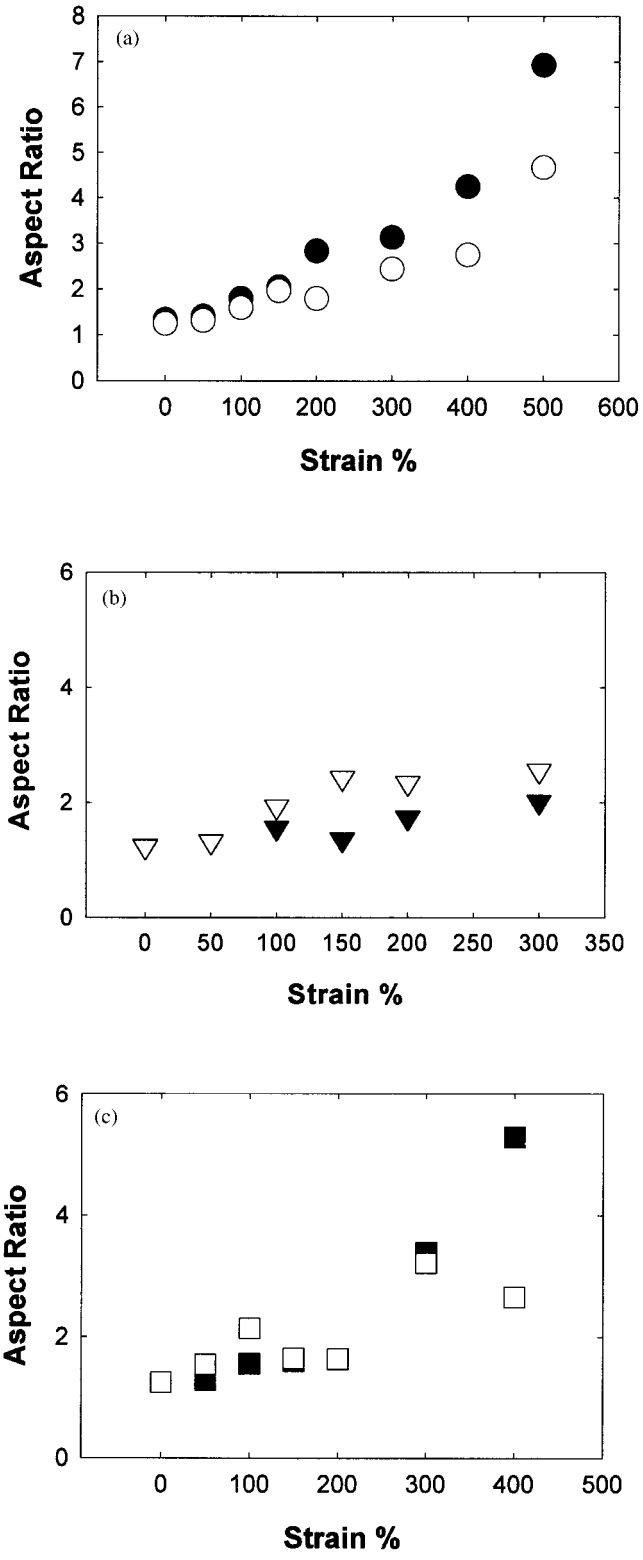

Figure 10 Air-hole aspect ratio of the calcite-filled (a) HDPE, (b) LDPE, and (c) LLDPE systems upon the (solid) second and (open) third mixing as a function of strain.

seems to show a better degree of mixing and degree of dispersion than those of the third mixing cycle.

The air-hole aspect ratio of the calcite-filled HDPE, LDPE, and LLDPE composites upon stretching was

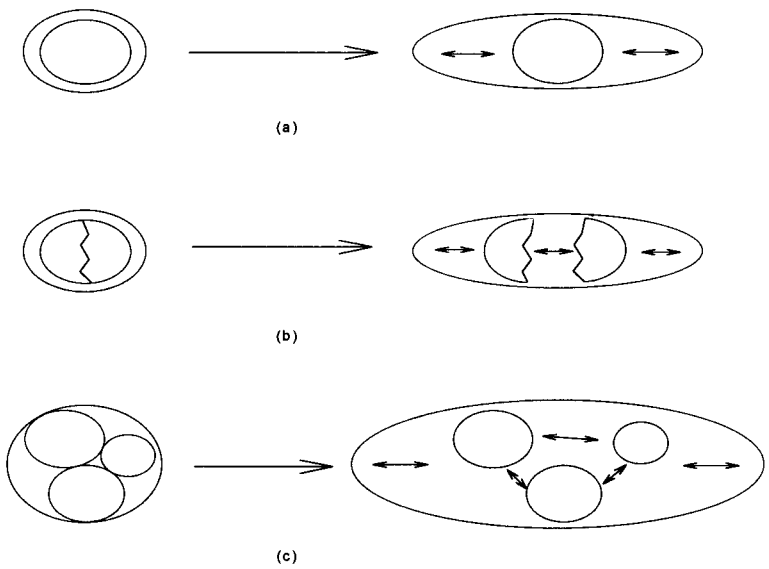

Figure 11 Schematic presentation of particle agglomerate variation for better degree of mixing (a) interface slippage; (b) particle breakup; (c) agglomerate breakup.

compared as a function of the mixing cycles (second and third mixings in this study) and is drawn in Figure 10(a–c), respectively. As seen in this figure, the air-hole aspect ratio of the specimen prepared between the second and third mixings was almost the same up to 150% of strain; However, it increased after 200% of strain. In particular, the aspect ratio of the specimen prepared in the second mixing dramatically increased up to 7.5 times at 500% stretching, which implies that the fibril structure and the breaking up of the HDPE matrix are the predominant behaviors at this range of stretching. On the other hand, for the LDPE system, the air-hole aspect ratio is gradually increased up to 300% elongation, but no significant difference between the second and the third mixings was observed upon further stretching. This may be caused by the change of the molecular weight and its distribution of the LDPE compound during TSE processing under high shear stress. However, the LLDPE system was unique. The aspect ratio of the LLDPE system prepared after the second and third mixings is about the same as that of LDPE up to 100% stretching, but after 150%, the trend of the variance of the aspect ratio is similar to that of HDPE after 200% stretching.

As we have seen from the previous figures, the dispersion and the degree of mixing of the calcite particles in the HDPE, LDPE, and LLDPE systems varied depending on not only the calcite agglomerate and its distribution, but also on the average air-hole diameter and the aspect ratio formed during mixing. Thus, we can propose a way of breaking up the calcite agglomerate for a better degree of mixing, as seen in Figure 11. The first is the interfacial slippage between the calcite particles and the PE matrix. The second will be the calcite particle breakup. The third may be the breakup of the calcite agglomerate into smaller particles. Similar phenomena were observed by others.[23,24]

CONCLUSIONS

The dependence of mixing cycles on the degree of dispersion and the degree of mixing of calcites in the HDPE, LDPE, and LLDPE matrices upon stretching was investigated using three different techniques: mechanical property, morphological behavior, and image analyzer analyses. The mechanical properties based on the tensile strength and maximum elongation exhibited that the second mixing would be the best for giving better properties in all systems. However, no significant difference between the second and third mixings was observed in the LDPE system. This seems to be related to the variation of the calcite agglomerate upon the mixing cycles. The morphological behavior of the three compounds were different, but it was hard to quantitatively differentiate the degree of mixing for various systems. The degree of mixing of the calcite-filled composites was analyzed by calculating the air-hole diameter in terms of the number-average, weight-average, and $z + 1$-average diameter upon various strain ratios. The overall average diameter of the air hole was almost the same regardless of the system, but the aspect ratio of the air hole varied significantly upon strain ratios and mixing cycles. In addition, a split of the calcite agglomerate or calcite particle breakup accelerated the air-hole propagation. Thus, the degree of dispersion and the degree of mixing seem to be influenced by the average calcite agglomerate size, the average diameter of the air hole, and the aspect ratio upon mixing cycles. Those factors would be originated by the difference in the chemical char-

acteristics upon various microstructures of PE, its molecular weight, and MWD. The shear stress imposed on the calcite compounds at high shear using a twin-screw extruder may also affect the different degrees of mixing.

The SK Corp. is appreciated by the authors for financially supporting this project. One of the authors (S.C.) especially thanks Inha University for providing special grants during 2000–2001. The authors also send gratitudes to the Institute of Polymer Engineering at the University of Akron for allowing the use of the image analysis instrument.

References

1. Kim, K. J.; White, J. L. J Ind Eng Chem 2001, 7, 1.
2. Kim, K. J. Dissertation University of Akron, 1998.
3. McNeish, A. A.; Byers, J. T. Low Rolling Resistance Tread Compounds-Some Compounding Solutions, Degussa Corp., ACS Rubber Division Meeting, Anaheim CA, May 1997.
4. Wang, Y.; Lu, J.; Wang, G. J Appl Polym Sci 1997, 64, 1275.
5. Suetsugu, Y.; White, J. L. J Appl Polym Sci 1983, 28, 1481.
6. Kim, K. J.; White, J. L. J Non-Newt Fluid Mech 1996, 66, 257.
7. Kim, K. J.; White, J. L. Polym Eng Sci 1999, 39, 2189.
8. Kim, K. J.; White, J. L.; Choe, S.; Dehennau, C. Polym Eng Sci, submitted for publication.
9. Harrington, E. A. Am J Soc 1927, 13, 467.
10. Chacko, V. P.; Karasz, F. E.; Farris, R. J. Polym Eng Sci 1982, 22, 968.
11. Chacko, V. P.; Farris, R. J.; Karasz, F. E. J Appl Polym Sci 1983, 28, 2701.
12. Banhegyi, G.; Karasz, F. E. J Polym Sci Polym Phys 1986, 24, 209.
13. Sheldon, R. P. Composite Polymeric Materials; Applied Science: London, 1982.
14. Wu, S. Polymer Interface and Adhesion; Dekker: New York, 1982.
15. Yosomiya, R.; Morimoto, K.; Nakajima, A.; Ikada, Y.; Toshio, S. Adhesion and bonding in Composites; Marcel Dekker: New York, 1990.
16. Lunt, J. M.; Shortall, J. B. Plast Rubber Process 1979, 4, 108.
17. Czarnecki, L.; White, J. L. J Appl Polym Sci 1980, 25, 1217.
18. Turkovich, R.; Erwin, L. Polym Eng Sci 1983, 23, 743.
19. Fisa, B. Plast Rubb Proc 1985, 6, 108.
20. Shon, K.; White, J. L. Polym Eng Sci 1999, 39, 1757.
21. Kwon, S.; Kim, K. J.; Kim, H.; Kim, T.; Lee, Y.; Lee, B. H.; Choe, S. Polymer, in press.
22. White, J. L. Rubber Processing: Technology, Materials, and Principles; Hanser: Cincinnati, 1995.
23. Li, J. X.; Hiltner, A.; Baer, E. J Appl Polym Sci 1994, 52, 269.
24. Xu, X. X.; Croccombe, A. D.; Smith, P. A. Int J Fatig 1994, 16, 469.